High-Resolution Mn EXAFS of the Oxygen-Evolving Complex in Photosystem II: Structural Implications for the Mn_4Ca Cluster

Junko Yano,[†‡] Yulia Pushkar,[†‡] Pieter Glatzel,[¶] Azul Lewis,[†] Kenneth Sauer,[†‡] Johannes Messinger,[‖] Uwe Bergmann,[⊥*] Vittal Yachandra[†*]

[†]*Melvin Calvin Laboratory, Physical Biosciences Division, Lawrence Berkeley National Laboratory, Berkeley, CA, 94720,* [‡]*Department of Chemistry, University of California, Berkeley, CA 94720,* [¶]*European Synchrotron Radiation Facility, BP 220, Grenoble Cedex, France 38043,* [‖]*Max-Planck-Institut für Bioanorganische Chemie, D-45470 Mülheim an der Ruhr, Germany,* [⊥]*Stanford Synchrotron Radiation Laboratory, Menlo Park, CA 94025.*

RECEIVED DATE (automatically inserted by publisher); VKYachandra@LBL.GOV

Photosynthetic water oxidation is a fundamental chemical reaction that sustains the biosphere and takes place at a catalytic Mn_4Ca site within photosystem II (PS II), which is embedded in the thylakoid membranes of green plants, cyanobacteria and algae.[1-3] The recent X-ray crystal structures with resolution between 3.2 and 3.8 Å[4-7] locate the electron density associated with the Mn_4Ca cluster in the multi-protein PS II complex, at different levels of detail. However, these resolutions do not allow an accurate determination of the positions of Mn[4-7] and Ca[6], or distances of Mn-Mn/Ca or the bridging and terminal ligand atoms; therefore, detailed structures critically depend on spectroscopic techniques such as EXAFS (extended X-ray absorption fine structure)[8-10] and EPR/ENDOR.[11-13] In addition, our recent studies with PS II crystals show that the Mn_4Ca site is highly susceptible to radiation damage; hence it is impossible to obtain meaningful Mn-Mn/Ca/ligand distances from XRD under the current conditions of X-ray dose and temperature.[14] EXAFS experiments require a lower X-ray dose than XRD; and radiation damage can be precisely monitored and controlled, thus allowing for data collection from an intact Mn cluster. EXAFS data also provide significantly higher Mn distance accuracy and resolution than the current 3.2 to 3.5 Å crystal structures.[15-17] Here we present data from a high-resolution EXAFS method using a novel multi-crystal monochromator (Fig. 1)[18] that can distinguish two distances that are apart by $\Delta R \geq 0.09$ Å with an accuracy of ~0.02 Å. These data resolve a distance heterogeneity in the short Mn-Mn distances of the S_1 and S_2 state and thereby provide firm evidence for three Mn-Mn distances between ~2.7 and ~2.8 Å. This result gives clear criteria for selecting and refining possible structures from the repertoire of proposed models based on spectroscopic and diffraction data.

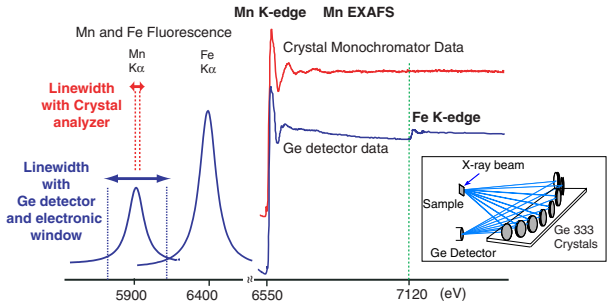

Figure 1. **Left:** A schematic representation of the detection scheme. Mn and Fe Kα1 and Kα2 fluorescence peaks are ~5eV wide and split by ~11eV (not shown). The multi-crystal monochromator with ~1 eV resolution is tuned to the Kα1 peak (red). The fluorescence peaks broadened by the Ge-detector with 150-200eV resolution are shown below (blue).[17] **Right:** The PS II Mn K-edge EXAFS spectrum from the S_1 state sample obtained with a traditional energy-discriminating Ge-detector (blue) compared, with that collected using the high-resolution crystal monochromator (red). Fe present in PS II does not pose a problem with the high-resolution detector (the Fe edge is marked by a green line). **Inset:** The inset shows the schematic for the crystal monochromator used in a backscattering configuration.[12]

The new detection technique results in significant improvement in metal-backscatterer distance resolution from EXAFS. In general, EXAFS spectra of systems which contain several different metals have a limited EXAFS range because of the presence of the rising edge of the next element, thus limiting the EXAFS distance resolution (see Suppl. material for details).[19] For the Mn K-edge EXAFS studies of PS II, the absorption edge of Fe in PS II limits the EXAFS energy range (Fig. 1). Traditional EXAFS spectra of PS II samples are collected as an excitation spectrum by electronically windowing the Kα fluorescence (2p to 1s, at 5899 eV) from the Mn atom.[15-17] The solid state detectors that have been used over the past decade have a resolution of about 150-200 eV (fwhm) at the Mn K-edge, making it impossible to discriminate Mn fluorescence from that of Fe Kα fluorescence (at 6391 eV). The presence of the obligatory 2-3Fe/PS II (Fe edge at 7120 eV) limits the data to a k-range of ~11.5 Å^{-1} (k=0.51$\Delta E^{1/2}$, the Mn edge is at 6540 eV and ΔE=580 eV) (Figs. 1 and 2 left). The Mn-Mn and Mn-ligand distances that can be resolved in a typical EXAFS experiment are given by $\Delta R = \pi/2k_{max}$, where k_{max} is the maximum energy of the photoelectron of Mn. The use of a high-resolution crystal monochromator allows us to selectively separate the Mn K fluorescence from that of Fe (Fig. 1), resulting in the collection of data to higher photoelectron energies and leading to increased distance resolution of 0.09 Å. The new detection scheme produces distinct advantages: 1) improvement in the distance resolution, and 2) more precise determination in the numbers of metal-metal vectors.

Earlier EXAFS studies of the S_1 and S_2 states of the OEC have shown that each Mn is surrounded by a first coordination shell of O or N atoms at 1.8 to 2.1 Å (peak I in Fig. 2), a second shell of short Mn-Mn distances at ~ 2.7 Å (peak II), and long Mn–Mn and Mn-Ca distances at ~3.3 Å (peak III).[8] These studies firmly established that the OEC in PS II is comprised of di-μ-oxo-bridged Mn_2 motifs characterized by a Mn-Mn distance of ~2.7 Å (peak II). However there was uncertainty about whether there are two or three di-μ-oxo-bridged Mn-Mn moieties,[20-22] because of the inherent error of the EXAFS method in the determination of the number of Mn-Mn vectors.[17] Range-extended EXAFS makes it possible to resolve and discriminate between the Mn-Mn distances contributing to peak II, facilitating a more accurate determination of the total number of interactions, because there must be an integral number of each of the resolved distances.

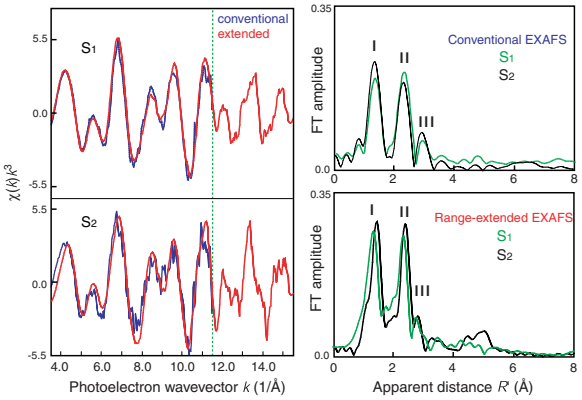

Figure 2. **Left:** k^3-weighted Mn EXAFS spectra from PS II samples in S_1 and S_2 states obtained with conventional EXAFS detection (blue) and with a high-resolution spectrometer (range-extended EXAFS, red). Green line at k=11.5 Å^{-1} denotes the spectral limit of conventional EXAFS imposed by the presence of the Fe K-edge. **Right**: Comparison of FTs of the Mn EXAFS spectra in conventional EXAFS collected up to the Fe edge at 11.5 Å^{-1} with range-extended EXAFS recorded up to 15.5 Å^{-1} in the S_1 (green) and S_2 states (black).

Fig. 2 shows the k^3-weighted Mn EXAFS spectra and the corresponding Fourier transforms (FT) of S_1 and S_2 states obtained using a solid-state Ge detector compared with the range-extended EXAFS data collected well past the Fe K-edge using a high-resolution crystal monochromator. The improvement in the range of the k-space data results in higher resolution and better precision in the fits.

Table 1 summarizes one and two Mn-Mn shell fits to peak II in the S_1 and S_2 states. The overall fit quality is monitored by comparing Φ and ε^2 parameters (for details see Suppl. material). There is significant improvement in the fit quality that contain two Mn-Mn distances of ~2.7 and ~2.8 Å over one-shell fits with an average Mn-Mn distance of ~2.74 Å. This is illustrated by two different two-shell fits in which N_1 and N_2 were fixed at different ratios: 1) N_1:N_2=1:1, corresponding to a scenario of two Mn-Mn interactions and 2) N_1:N_2=2:1, corresponding to three Mn-Mn interactions. The latter case is clearly preferable based on the quality of the fits to both the S_1 and S_2 state data.

The current observation by range-extended EXAFS supports models that contain three Mn-Mn vectors; two at ~2.7 Å and one at ~2.8 Å. Models for the Mn cluster compatible with these parameters and containing one or two Mn-Mn interactions at 3.3 Å are shown in Fig. 3.

Preliminary studies using oriented PS II membranes show much better resolution for Fourier peak III and raise the possibility of resolving the Mn-Mn/Ca contributions in future studies using this high-resolution EXAFS methodology. In conclusion, two Mn-Mn distances of 2.73 and 2.82 Å in a 2:1 ratio can be resolved using this new method proving the presence of three short Mn-Mn vectors in the S_1 and S_2 states of the Mn_4Ca cluster.

Table 1 One- and Two-Shell Fits of Fourier Peak II from Range-Extended EXAFS data from the S_1 and S_2 States.

		R(Mn-Mn), (Å)	N	σ^2*10^3 (Å)^2	Φx10^3	ε^2x10^5
S_1 State	One Shell	2.72	1.21	3.0	0.18	0.060
	Two Shells	2.68	0.60	1.0	0.16	0.054
	N_1:N_2=1:1	2.77	0.60	1.0		
	N_1:N_2=2:1	2.71	0.87	1.0	0.11	0.035
		2.81	0.44	1.0		
S_2 State	One Shell	2.75	1.20	2.6	0.13	0.042
	Two Shells	2.71	0.60	1.0	0.11	0.038
	N_1:N_2=1:1	2.79	0.60	1.0		
	N_1:N_2=2:1	2.73	0.84	1.0	0.09	0.031
		2.82	0.42	1.0		

N_1 and N_2 are the numbers of interactions for two shells with fixed σ^2 (Debye-Waller parameter). Φ and ε^2 are fit-quality parameters; for details see Suppl. material.

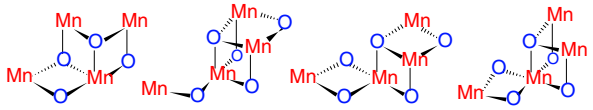

Figure 3. Models for the Mn_4Ca complex (Ca not shown) compatible with the high resolution Mn EXAFS data with three short 2.7 - 2.8 Å Mn-Mn distances and one or two longer Mn-Mn distances at ~3.3 Å.

Acknowledgment. We thank Stephen Cramer for suggesting the range-extended EXAFS experiment and for providing access to the crystal analyzer. This work was supported by the NIH Grants GM-55302 (VKY), GM-65440 (SPC), NSF grant CHE-0213592 (SPC), and by the Director, Office of Science, Basic Energy Sciences, Division of Chemical Sciences, Geosciences, and Biosciences (VKY) and Office of Biological and Environmental Research (SPC) of the Department of Energy under Contract DE-AC03-76SF00098. JM was supported by the DFG (Me 1629/2-3). Synchrotron facilities were provided by APS, Argonne operated by DOE, Office of Basic Energy Sciences under contract W-31-109-ENG-38. BioCAT is a NIH-supported Research Center RR-08630.

Supporting Information Available: High-resolution EXAFS methodology and description of the EXAFS simulations. This material is available free of charge via the Internet at http://pubs.acs.org.

References

(1) Debus, R. J. *Biochim. Biophys. Acta* **1992**, *1102*, 269-352.
(2) Rutherford, A. W.; Zimmermann, J.-L.; Boussac, A. In *The Photosystems: Structure, Function, and Molecular Biology*; Barber, J., Ed.; Elsevier B. V.: Amsterdam, 1992; pp 179-229.
(3) Ort, D. R.; Yocum, C. F., Eds. *Oxygenic Photosynthesis: The Light Reactions*; Kluwer Academic Publishers: Dordrecht, 1996.
(4) Zouni, A.; Witt, H.-T.; Kern, J.; Fromme, P.; Krauß, N.; Saenger, W.; Orth, P. *Nature* **2001**, *409*, 739-743.
(5) Kamiya, N.; Shen, J. R. *Proc. Natl. Acad. Sci. USA.* **2003**, *100*, 98-103.
(6) Ferreira, K. N.; Iverson, T. M.; Maghlaoui, K.; Barber, J.; Iwata, S. *Science* **2004**, *303*, 1831-1838.
(7) Biesiadka, J.; Loll, B.; Kern, J.; Irrgang, K. D.; Zouni, A. *Phys. Chem. Chem. Phys.* **2004**, *6*, 4733-4736.
(8) Yachandra, V. K.; Sauer, K.; Klein, M. P. *Chem. Rev.* **1996**, *96*, 2927-2950.
(9) Penner-Hahn, J. E. *Struct. Bond.* **1998**, *90*, 1-36.
(10) Sauer, K.; Yano, J.; Yachandra, V. K. *Photosynth. Res.* **2005**, *85*, 73-86.
(11) Peloquin, J. M.; Britt, R. D. *Biochim. Biophys. Acta* **2001**, *1503*, 96-111.
(12) Hasegawa, K.; Ono, T.-A.; Inoue, Y.; Kusunoki, M. *Chem. Phys. Lett.* **1999**, *300*, 9-19.
(13) Kulik, L. V.; Epel, B.; Lubitz, W.; Messinger, J. *J. Am. Chem. Soc.* **2005**, *127*, 2392-2393.
(14) Yano, J.; Kern, J.; Irrgang, K.-D.; Latimer, M. J.; Bergmann, U.; Glatzel, P.; Pushkar, Y.; Biesiadka, J.; Loll, B.; Sauer, K.; Messinger, J.; Zouni, A.; Yachandra, V. K. *Proc. Natl. Acad. Sci. USA* **2005**, *102*, 12047-12052.
(15) Scott, R. A. In *Structural and Resonance Techniques in Biological Research*; Rousseau, D. L., Ed.; Academic Press: Orlando, 1984; pp 295-362.
(16) Cramer, S. P. In *X-ray Absorption: Principles, Applications and Techniques of EXAFS, SEXAFS, and XANES*; Koningsberger, D. C., Prins, R., Eds.; Wiley-Interscience: New York, 1988; pp 257-320.
(17) Yachandra, V. K. *Methods Enzymol.* **1995**, *246*, 638-675.
(18) Bergmann, U.; Cramer, S. P. In *SPIE Conference on Crystal and Multilayer Optics*; SPIE: San Diego, CA, 1998; Vol. 3448, pp 198-209.
(19) Glatzel, P.; de Groot, F. M. F.; Manoilova, O.; Grandjean, D.; Weckhuysen, B. M.; Bergmann, U.; Barrea, R. *Phys. Rev. B: Condens. Matter* **2005**, *72*, Art. Number 014117.
(20) Robblee, J. H.; Messinger, J.; Cinco, R. M.; McFarlane, K. L.; Fernandez, C.; Pizarro, S. A.; Sauer, K.; Yachandra, V. K. *J. Am. Chem. Soc.* **2002**, *124*, 7459-7471.
(21) Dau, H.; Iuzzolino, L.; Dittmer, J. *Biochim. Biophys. Acta* **2001**, *1503*, 24-39.
(22) Kusunoki, M.; Takano, T.; Ono, T.; Noguchi, T.; Yamaguchi, Y.; Oyanagi, H.; Inoue, Y. In *Photosynthesis: from Light to Biosphere*; Mathis, P., Ed.; Kluwer Academic Publishers: Dordrecht, The Netherlands, 1995; Vol. II, pp 251-254.

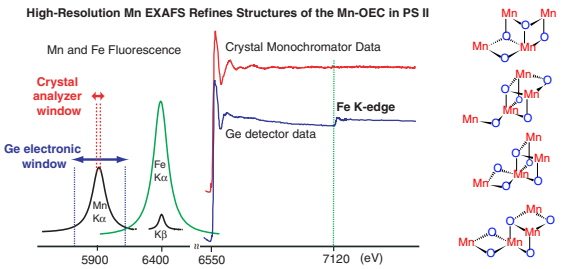

The biological generation of oxygen by the oxygen-evolving complex in photosystem II (PS II) is one of nature's most important reactions. The recent X-ray crystal structures, while limited by resolutions of 3.2 to 3.5 Å, have located the electron density associated with the Mn_4Ca complex within the multi-protein PS II complex. Detailed structures critically depend on input from spectroscopic techniques such as EXAFS and EPR/ENDOR, as the XRD resolution does not allow for accurate determination of the position of Mn/Ca or the bridging and terminal ligand atoms. The number and distances of Mn-Mn/Ca/ligand interactions determined from EXAFS provide important constraints for the structure of the Mn cluster. Here we present data from a high-resolution EXAFS method using a novel multi-crystal monochromator that show three short Mn-Mn distances between 2.7 and 2.8 Å and hence the presence of three di-μ-oxo bridged units in the Mn_4Ca cluster. This result imposes clear limitations on the proposed structures based on spectroscopic and diffraction data and provides input for refining such structures.